Supplemental Information

A computationally designed inhibitor of an Epstein-Barr viral Bcl-2 protein induces apoptosis in infected cells

Erik Procko, Geoffrey Y. Berguig, Betty W. Shen, Yifan Song, Shani Frayo, Anthony J. Convertine, Daciana Margineantu, Garrett Booth, Bruno E. Correia, Yuanhua Cheng, William R. Schief, David M. Hockenbery, Oliver W. Press, Barry L. Stoddard, Patrick S. Stayton, and David Baker.

Supplemental Information Index

1. Supplementary Figures S1-S7
2. Supplementary Tables S1-S5
3. Extended Experimental Procedures
4. Supplemental References

Supplementary Table S3 is available online in a separate spreadsheet file. A bzipped tar archive file of design PDBs, related to Figure 1, is also provided online.

Supplementary Figures and Tables

Supplementary Figure S1, related to Figure 1. Computational design of BHRF1 binders using side chain grafting or *de novo* protein assembly (Fold From Loops) methods.
(A) Side chain grafting protocol. A helix of a scaffold protein (orange) is structurally aligned using PyMOL to the Bim-BH3 motif (blue) bound to BHRF1 (green) from the Bim-BH3•BHRF1 crystal structure (PDB 2WH6) (i). Residues of Bim-BH3 that interact with BHRF1 are "grafted" to the aligned scaffold helix via mutagenesis (ii); the scaffold now presents a binding surface to BHRF1, with critical interactions at the interface borrowed from Bim-BH3. The remainder of the interface is designed to minimize the energy of the bound scaffold•BHRF1 complex using RosettaDesign (iii). Scaffold residues within 8 Å of the interface can be mutated to all possible amino acids except pro/cys, while BHRF1 side chains can repack to alternative rotamers. See Table S1.
(B) *De novo* protein assembly protocol using ROSETTA Fold From Loops. A guiding scaffold (grey ribbon) is aligned to the Bim-BH3 motif (blue) bound to BHRF1 (green) (i). Bim-BH3 acts as a folding nucleus; the peptide is extended on both ends and a new protein structure (orange) is built using fragment-based assembly (ii), followed by multiple rounds of minimization and sequence design. The scaffold simply guides the assembly process based on atom pair distance constraints and topology. The newly assembled protein is docked to BHRF1 via the incorporated Bim-BH3 motif, and the surrounding interface is designed (iii) as described in (A). Many designs are generated, each with unique sequence and structure, that are filtered based on multiple criteria (iv). See Table S2.

Supplementary Figure S2, related to Figure 1. Predictions of folding probability correlate with designed protein functionality.

(A) Ribbon representation of protein Index-21 (orange) bound to BHRF1 (green). Index-21, which fails to bind BHRF1, was human-modified to give design BbpD04, which binds BHRF1 with nanomolar affinity. The human-made mutations introduced into computational precursor Index-21 to form BbpD04 are indicated with black labels, and the side chains of substituted residues are shown as spheres. BbpD04 contained 15 human-introduced mutations (out of 116 residues total) which increase packing within the hydrophobic core and the hydrophilicity of the exposed surface.

(B) Structures of designs that bound BHRF1 (Indexes-00 to 04) are aligned via the Bim-BH3 incorporation motif (boxed with broken line). Side view showing structural diversity. Index-00, orange; Index-01, blue; Index-02, yellow; Index-03, green; Index-04, magenta.

(C) As in (B), viewed from N-terminus.

(D) Sequence alignment of BHRF1-binding designs (Indexes-00 to 04) and the guiding scaffold (3LHP chain S). Amino acid identity (black shading) or chemical similarity (grey shading) to design Index-00/BbpD04 is shown, illustrating sequence diversity. The Bim-BH3 incorporation site is marked with a red bar above.

(E) Putative binders (Indexes-01 to 04) were expressed individually on the yeast surface and validated by titrating the concentration of biotinylated BHRF1 to determine apparent binding affinities. Three randomly chosen designs that are highly expressed but do not bind based on the selection data did not show interactions with BHRF1.

(F-H) Properties of the designed interfaces plotted against the experimental enrichment ratios after selection for binding to 100 nM BHRF1. Each data point (black diamonds) represents a designed protein (Indexes-01 to 74) bound to BHRF1. Designs that are positively enriched bind BHRF1. Plotted are the (F) interface buried solvent-accessible surface area (SASA), (G) the calculated interface binding energy ($\Delta\Delta G$), and (H) the number of unsatisfied buried polar atoms at the interface. Keeping in mind that designs have already undergone some quality filtering which would remove those that score exceedingly poorly on any of these metrics, amongst the experimentally tested computational designs there is no general trend between these interface metrics and binding to BHRF1.

(I-K) As for (F-H), except showing computed metrics for the unbound designed proteins. Plotted are enrichment ratios versus (I) the holes score of the apo-protein (an indicator of packing within the core), (J) calculated folding energy, and (K) unsatisfied buried polar atoms. Again, none of these metrics is predictive of which of the experimentally tested designs bind BHRF1.

(L) Examples of "forward folding" landscapes for BHRF1-binding designs. Proteins indexes-00, 01 and 04 bind BHRF1. Proteins indexes-15, 47 and 67 do not interact with BHRF1 based on the selection data in main Fig. 1. 30,000-100,000 conformations were generated using ROSETTA-based *ab* initio structure prediction for each query (black points). 40 relaxed conformations were generated for each target computational model (red points). Cα-Cα RMSD is measured between each predicted conformation and the intended computational model. An ideal protein would have an energy funnel from distant high-energy conformers towards a single low energy folded state (as in Indexes-00, 01 and 04), and therefore a small RMSD between the lowest energy predicted structures and the intended designed conformation.

Supplementary Figure S3, related to Figure 2. The interaction of BbpD04.2 with BHRF1 in solution is diminished by a mutation within the hydrophobic interface.
(A) In the left panel, BbpD04.2 (black trace) forms a left-shifted higher MW complex (orange) when mixed with BHRF1 (grey). In the right panel, BbpD04.2 L54E (black) with a mutation in the binding site does not shift (orange) when mixed with BHRF1 (grey). The BINDI L54E mutation is based on the observation that the equivalent mutation to Bim, L62E, severely diminishes binding of Bim-BH3 to all Bcl-2 family members shown in panels (B-J) below.
(B) Bim-BH3 (blue cartoon) bound to BHRF1 (green) from crystal structure 2WH6. L62 of Bim-BH3 is buried within the hydrophobic interface.
(C-J) Bim-BH3 wildtype (red) or L62E mutant (black) were expressed on the yeast cell surface. The cells were incubated with biotinylated ligand, washed, and stained with anti-myc-FITC to detect expression (FL1 fluorescence) and streptavidin-PE to detect bound ligand (FL2 fluorescence). Shown are representative flow cytometry plots from two repeats. Yeast were incubated without ligand (C), or with 10 nM BHRF1 (D), Bcl-2 (E), Bfl-1 (F), Bcl-w (G), Mcl-1 (H), Bcl-X_L (I) or Bcl-B (J).

Supplementary Figure S4, related to Figure 2. Mutagenesis of an internal cysteine allows site-specific conjugation with cysteine-modifying agents at the termini.
(A) Short peptide linkers containing single cysteines were genetically fused to the BbpD04.2 termini. Linker-3 termini were used in all experiments described in the main text where conjugation to a cysteine was required.
(B) Cysteine-linkers at either N- or C-termini reacted rapidly in seconds with 5kD polyethylene glycol (PEG)-maleimide (Creative PEGWorks), producing a higher MW product with reduced electrophoretic mobility. Purified proteins (100 µg/ml) were incubated on ice in reaction buffer (50 mM Tris [pH 7.5], 150 mM NaCl) with 0.5 mM reagent. Reactions were stopped with DTT (0.1 M final) and analyzed on Coomassie-stained sodium dodecylsulphate (SDS)-polyacrylamide gels. BbpD04.2 has its own buried cysteine (C103), which becomes exposed for PEG-maleimide conjugation in the presence of the harsh detergent SDS, indicating the protein is folded and the hydrophobic core is generally shielded from solvent unless chemically denatured.
(C) Cysteine-linker BbpD04.2 proteins (200 µM) were conjugated to HPDP-biotin (0.4 mM; from a 4 mM stock dissolved in DMSO; Thermo Scientific) for 4 h at room temperature in PBS containing 1 mM EDTA. Excess HPDP-biotin was removed with a 700 µl desalting column (Thermo Scientific). Biotinylated protein (50 µM) was incubated with tetrameric streptavidin (12.5 µM) in PBS / 1 mM EDTA, and aggregation measured by absorbance at 350 nm. We hypothesized that, in addition to the exposed terminal cysteine, the internal cysteine was weakly conjugated under these conditions to form aggregated streptavidin-complexes. Mutation of the internal cysteine (C103A) markedly diminishes aggregation under the same conditions.
(D) DMSO, the solvent used for dissolving HPDP-biotin, did not increase exposure of the internal cysteine for PEG-maleimide modification. Compare to the effect of SDS, a denaturant, in panel B. Reaction conditions were as described in (B), for 600 s.
(E) PEG-maleimide reacted with a fraction of the BbpD04.2 protein when incubated together overnight at room temperature (RT). Reaction described in (B).
(F) As described in panels above, the internal cysteine is poorly reactive compared to exposed terminal cysteines, but its undesired conjugation to modifying agents during longer incubations at room temperature nonetheless necessitated its removal. Both BbpD04.2 C103A and C103V mutations were predicted by the ROSETTA energy function to be tolerated following minimization. BbpD04.2 C103V had reduced specificity by yeast surface display for BHRF1 over other prosurvival Bcl-2 proteins, whereas BbpD04.2 C103A (called BbpD04.3) had only a minor loss of affinity and specificity, and was therefore chosen for further experiments.

Supplementary Figure S5, related to Figure 2. BINDI has increased bacterial expression and protein stability than the original design.
(A) BbpD04.3 point mutants were expressed in *E. coli* Rosetta 2 cells overnight at 22 ºC, after induction at an OD_{600} ~ 1.0 with 0.15 mM IPTG. E. coli Rosetta 2 express tRNAs for rare codons, and were found to have lower expression than an alternative E. coli BL21 (DE3) strain. This provided greater contrast between expression levels of mutants in this experiment. Cells were harvested, the C-terminally 6his-tagged proteins precipitated with NiNTA-agarose to partially remove background bands, and analyzed on Coomassie-stained SDS-polyacrylamide electrophoretic gels. White arrows indicate mutations with elevated expression. Shown are representative results from 2-3 repeats.
(B) As in (A), with mutations now combined to provide a large increase in expression.
(C) Computational model of BbpD04.3 (orange) bound to BHRF1 (green). Combined mutations in variant BINDI that improved expression are in dark blue stick representation. Mutations are described in main text.
(D) Molar ellipticity at 222 nm as the protein (40 µM in PBS) is heated from 25 ºC to 95 ºC (dark colored lines), and cooled from 95 ºC back to 25 ºC (light colored lines). Substantial helical structure remains at 95 ºC. Evolved variants BbpD04.3 (pink) and BINDI (green) fully renature. Original design BbpD04 (blue) has a more linear melt curve, and a fraction of the protein precipitates upon heating and fails to refold when cooled.
(E) Molar ellipticity of original design BbpD04 as a function of wavelength. CD spectra were recorded at 25 ºC (black), 95 ºC (red), and after cooling the sample back to 25 ºC (grey).
(F) As in (E), measured for variant BbpD04.3.
(G) As in (E), measured for variant BINDI.
(H) Protease-susceptibility of original design BbpD04 and affinity-matured variants BbpD04.3 and BINDI. Protein substrates were incubated for 0, 5, 15, 30, 60, and 120 minutes with protease at 37 ºC, reactions were terminated with protease inhibitors, and substrate hydrolysis followed by observing the decrease in full-length protein on Coomassie-stained SDS-polyacrylamide gels. Shown are representative results from 3 repeats.

Supplementary Figure S6, related to Figure 4. The crystal structure of BHRF1-bound BINDI at 2.05 Å resolution.
(A) The asymmetric unit contains two copies of BHRF1•BINDI: BHRF1 chains A and C are dark and light green, respectively, and BINDI chains B and D are dark red and orange, respectively.
(B) Ribbon representations of the two copies in the asymmetric unit are colored as in (A) and superimposed. Since the two copies are nearly identical, only BHRF1 chain C and BINDI chain D are shown in main Figure 4 and subsequent panels.
(C) Close-up view of BHRF1 loop 92-97. The crystal structure of BHRF1 (green)-bound BINDI (orange) is overlaid with the crystal structure of BHRF1 (purple) bound to Bim-BH3 (pale blue). An arrow indicates the outwards motion of BHRF1 loop 92-97 when BINDI occupies the ligand-binding site. Loop motion is possibly due to proximity of designed BINDI residue Met55; loop relocation allows hydrogen bonding to solvent.
(D) As in (C), showing a close-up view of the outwards motion of BHRF1 loop 74-78 when BINDI is bound. Designed BINDI residue Arg53 intrudes into the space this loop occupies in the Bim-BH3•BHRF1 structure.
(E) Crystal structure of BINDI (grey surface) bound to BHRF1 (green). The buried contact surface areas are indicated below.
(F) The surface of BINDI, in the same orientation as in (E), with the buried contact surface colored. Buried residues that were taken from the incorporated Bim-BH3 motif used to seed design are magenta (also see panel H). Buried residues that were designed in the surrounding contact surface are blue.
(G) Residues of BINDI that changed during affinity maturation are red. Only two residues at the edge of the incorporated Bim-BH3 motif were substituted (W49Y and F61Y).
(H) Sequences of the Bim-BH3 motif and equivalent regions in BbpD04 and BINDI. Residues of Bim-BH3 that were fixed in the design of BbpD04 are shaded magenta. Residues that changed during affinity maturation to generate BINDI are shaded red. Based on these sequences, four 26-residue peptides were fused to the C-terminus of maltose-binding protein (MBP): BbpD04“BH3”, BINDI“BH3”, BimBH3-W57Y-F69Y and BimBH3-5*. The latter two peptides have mutations to the Bim-BH3 motif based on changes during affinity maturation of BINDI, either just in the residues directly taken from Bim or across the entire 26 residue region.
(I) MBP-peptide fusions were tested by BLI for binding to Bcl-2 proteins. Compare to main Figure 3C-E. None of the peptides had the affinity or specificity for BHRF1 of BINDI.

Supplementary Figure S7, related to Figures 5 and 6. Control experiments for analyses of BINDI activity.
(A) Mitochondria were harvested from Ramos (grey) and Ramos-AW (crimson) cells and treated with the negative controls Bim-BH3 L62E, BINDI L54E and the inactive scaffold 3LHP(S). Released cytochrome c was quantified by ELISA. Mean ± SD, n = 4.
(B) In the upper insert, the crystal structure of BINDI (orange) bound to BHRF1 (green) shows the interaction of Asn62 with the N-terminus of helix α6. Below, BINDI mutation N62S (dark blue) is predicted to maintain interface interactions.
(C) Mitochondria were isolated from three EBV-negative and five EBV-positive B cell cancer lines, and were treated with 10 μM positive control Bim-BH3 peptide (grey bars) or 10 μM negative control 3LHP(S) (green bars). Released cytochrome c was quantified by ELISA, mean ± SD, n = 4. Below, gene expression was qualitatively analyzed by reverse transcription-PCR for EBV BHRF1 and endogenous human GAPDH. PCR products were separated on agarose electrophoretic gels.
(D) Cells were incubated with 4 μM antennapedia peptide-fusions of BINDI, BINDI-L54E or 3LHP chain S. Cell viability after 24 h was assessed by quantifying metabolic activity. Results are representative of two independent experiments, each in triplicate; mean ± SD is shown.
(E) Mean change in mouse body weight ± SD for the treatment groups in main Figure 6. Treatment is given on days 0, 3 and 6 (black arrows). Treatment groups are untreated/PBS control (black), chemo-only (grey), copolymer:αCD19:3LHP(S) with chemo (green) and copolymer:αCD19:BINDI with chemo (orange).

Supplementary Table S1, related to Figure 1. Summary of designs based on a side chain grafting strategy.

Table S1. Summary of designs based on a side chain grafting strategy.				
Design Name	**Scaffold**	**Grafted Bim-BH3 Residues †**	**Designed Residues †**	**K_D BHRF1 ¶**
BbpG1	3LHP(S)	V55W, R56I, G57A, E60L, R63I, V64G, A65D, R67F	None	–
BbpG1.D			E45D, E46Q, I48K, K49H, D50Q, L52V, K53H, I54Y, E58L, Q61E, R71E, T102R, D103W, I106F, K107Q, E110T, L113A, A114K, E117A, L120A, T121Q	–
BbpG2		S10P, D11E, R13W, K14I, D15A, V18L, D21I, K22G, A23D, E25F, A26N	None	> 100 nM
BbpG2.D			E17K, R19A, N29L, K33A, N68R, V69A, D72A, K76N	60 ± 8 nM
BbpG3	3FBL	D97I, M98A, E101L, N104I, N105G, A106D, S107F, A108N	None	–
BbpG3.D			K84E, S85D, M89A, S95H, S96E, A100R, Y102M	70 ± 20 nM
BbpG4	1LP1	S41W, A42I, N43A, A46L, K49I, K50G, L51D, D53F	None	–
BbpG4.D			F5H, K7D, E8D, V11K, E15S, Q40R, L45A, E47M, A54D	81 ± 8 nM
BbpG5		A42P, L45W, A46I, E47A, K50L, D53I, A54G, Q55D	None	–
BbpG5.D			Q26E, S33D, Q40R, K49R, L51M, A56S, K58L	–
BbpG6		D24P, P25E, K27W, K28I, F32L, W35I, D36G	None	–
BbpG6.D			V17A, I31A, S33M	–

† The native scaffold residue (identity and number) is given first, followed by the amino acid type it was mutated to.
¶ Apparent K_D as measured by yeast display titrations. The design is yeast surface expressed, and BHRF1 is soluble.

Supplementary Table S2, related to Figure 1. Summary of designs based on *ab initio* fragment assembly of a *de novo* protein around a folding nucleus.

Table S2. Summary of designs based on a seeded *ab initio* fragment assembly strategy.				
Design Name	**Topology Guide**	**Site †**	**Expressed and soluble in *E. coli* ¶**	**Binds 400 nM BHRF1 ***
BbpD01 (S103A)	3LHP(S)	Bim: 56-70 Scaffold: 54-68	– (–)	
BbpD02			–	
BbpD03 (A60V)			– (–)	
BbpD04			+	Yes: 58 ± 3 nM
BbpD05			–	
BbpD06			+	No
BbpD07			+	Yes: 60 ± 10 nM
BbpD08	1LP1	Bim: 52-67 Scaffold: 40-55	–	
BbpD09			–	
BbpD10 (S13V A45C) (S13V A45C E25A)		Bim: 54-66 Scaffold: 24-36	+ (+) (+)	No (No) (No)
BbpD11			–	
BbpD12 (E25V)			+ (+)	No (Yes: weak)
BbpD13 (E25A)			+ (–)	No
BbpD14			–	
BbpD15 (K10S V28A)			– (–)	
BbpD16 (I10N V27A)			– (–)	
BbpD17			+	No

† Indicates the region of Bim-BH3 from crystal structure 2WH6 that was used to nucleate *ab initio* folding, and the site within the topology guide where the Bim-BH3 folding nucleus was located.

¶ E. coli BL21(DE3) cells cultured in terrific broth to an OD(600 nm) ~0.5 were induced with 0.1 mM IPTG overnight at 20 °C and protein expression investigated by SDS-PAGE.

* Designs were expressed on the yeast surface and incubated with 400 nM monomeric BHRF1-biotin, washed, and stained with anti-myc-FITC (expression) and streptavidin-PE (binding).

Supplementary Table S3, related to Figure 1. Sequences of seeded *ab initio* designs tested by high throughput library sorting.

Please see accompanying spreadsheet file online.

Supplementary Table S4, related to Figure 2. Mutations to BbpD04 to enhance electrostatic complementarity with BHRF1 and increase specificity.

Predicted differences in binding energies to BHRF1 and Mcl-1 (ΔΔG, in ROSETTA energy units or REU) were calculated by modifying the ROSETTA energy function to down-weight repulsive interactions and add Poisson-Boltzmann electrostatics. Experimental differences in binding energies were determined from apparent yeast display K_Ds (mean from n = 3-6).

Table S4. BbpD04 mutations based on predicted long-range electrostatics

BbpD04 Mutation	**PREDICTION** $\Delta\Delta G_{BHRF1} - \Delta\Delta G_{Mcl-1}$ **(REU)**	**EXPERIMENT** $\Delta\Delta G_{BHRF1} - \Delta\Delta G_{Mcl-1}$ **(kJ / mol)**
E40Q	-3.37	-0.58
R43K	-5.09	> 0
E48K	-3.18	0.63
E48R	-4.30	-3.19
K31E E48R		-1.93
E65R	-5.45	-3.01
H104K	-7.80	-0.40
D105I	-3.80	-0.91
D105K	-10.11	-1.23
Q111K	-9.99	0.18
K31E E48R E65R (BbpD04.1)		-6.25

Supplementary Table S5, related to Figure 4. Crystallographic data collection and refinement statistics.

Table S5. Crystallographic data collection and refinement statistics.	
Data Collection	
Wavelength (Å)	1.001
Space group	$p2_1$
a (Å)	52.07
b (Å)	113.67
c (Å)	56.16
b (°)	90.11
Resolution (Å)	38.4-2.05
Unique reflections	40233
Redundancy*	2.7 (2.2)
Completeness (%)*	97.9 (89.8)
I/σ*	10.7 (4.0)
Rmerge [a] (%)*	6.6 (32.6)
B(iso)(Å^2)	25.9
Twinning operator	-h, -k, l
Twinning fraction	0.550
Refinement	
Protein atoms	4259
Solvent molecules	17
R-factor[b] (%)*	0.173
R-free[b] (%)*	0.227
RMSD: Bond length (Å)	0.011
RMSD: Angles (°)	1.459
Ramachandran (%)	
Favorable region	96.76
Allowed region	2.48
Outliers	0.76

* Highest resolution shell values in parentheses.

[a] Rmerge = $\sum|I_{hi} - \langle I_h \rangle|/\sum I_{h,}$ where I_{hi} is the *i*th measurement of reflection h, and $\langle I_h \rangle$ is the average measured intensity of reflection h.

[b] R-factor/R-free = $\sum_h|F_{h(o)} - F_{h(c)}|/ \sum_h|F_{h(o)}|$, where R-free was calculated with 5% of the data excluded from refinement.

Extended Experimental Procedures

Computational methods: General information

ROSETTA software can be downloaded from https://www.rosettacommons.org/ and is available free to academic users. Online documentation can be found at https://www.rosettacommons.org/manuals/archive/rosetta3.5_user_guide/index.html and instructions for RosettaScripts syntax is available at https://www.rosettacommons.org/manuals/archive/rosetta3.3_user_guide/RosettaScripts_Documentation.html.

Computational methods: Side chain grafting on a fixed backbone

Input Files
A suitable helical region of the scaffold protein was aligned to the Bim-BH3 motif of PDB 2WH6 (Bim-BH3•BHRF1) using PyMOL (Schrödinger, LLC). The structural alignment was visually inspected for minimal backbone clashes between the scaffold protein and BHRF1 (side chain clashes may be fixed later by sequence design of the scaffold and by rotamer repacking on the target). Based on the structural alignment, scaffold residues were mutated in PyMol to the corresponding Bim-BH3 residue within the interface core; this 'grafted' important Bim interaction residues to the scaffold surface by mutation. A new PDB file containing the partially mutated scaffold bound to BHRF1 was saved and used as the input for ROSETTA-based design.

Design within ROSETTA
An example command line to launch ROSETTA (Leaver-Fay et al., 2011) and example recipe/protocol file (Fleishman et al., 2011b) are as follows:

```
/directory_path/rosetta_scripts.static.linuxiccrelease -database
/directory_path/minirosetta_database/ -parser:protocol protocol.xml -s
input_structure.pdb -nstruct 10 -ntrials 5 -ignore_unrecognized_res -ex1 -ex2
-extrachi_cutoff 5 -hbond_fade 1.9 2.3 2.3 2.6 0.3 0.7 0.0 0.05 -
no_his_his_pairE

<dock_design>
<SCOREFXNS>
</SCOREFXNS>
<TASKOPERATIONS>  These list the grafted Bim-BH3 residues to remain fixed.
    <ProteinInterfaceDesign name=pido/>
    <RestrictResidueToRepacking name=fix_47 resnum=204/>
    <RestrictResidueToRepacking name=fix_48 resnum=205/>
    <RestrictResidueToRepacking name=fix_51 resnum=208/>
    <RestrictResidueToRepacking name=fix_54 resnum=211/>
    <RestrictResidueToRepacking name=fix_55 resnum=212/>
    <RestrictResidueToRepacking name=fix_56 resnum=213/>
    <RestrictResidueToRepacking name=fix_58 resnum=215/>
    <RestrictResidueToRepacking name=fix_59 resnum=216/>
</TASKOPERATIONS>
<FILTERS>
    <Ddg name=ddg_loose scorefxn=score12 threshold=-2/>
    <Ddg name=ddg_strict scorefxn=score12 threshold=-15/>
```

```
    <Sasa name=sasa threshold=800/>
    <BuriedUnsatHbonds name=unsat cutoff=20/>
</FILTERS>
<MOVERS>
    <Docking name=dck score_high=score12 fullatom=1 local_refine=1/>
    <build_Ala_pose name=ala_pose partner1=0 partner2=1
task_operations=fix_47,fix_48,fix_51,fix_54,fix_55,fix_56,fix_58,fix_N59,pido
/>
    <Prepack name=ppk scorefxn=score12 jump_number=0
task_operations=fix_47,fix_48,fix_51,fix_54,fix_55,fix_56,fix_58,fix_59pido/>
    <RepackMinimize name=design scorefxn_repack=score12
scorefxn_minimize=score12 repack_partner1=1 repack_partner2=1
design_partner1=0 design_partner2=1 interface_cutoff_distance=8.0
minimize_bb=1 minimize_rb=1 minimize_sc=1
task_operations=fix_47,fix_48,fix_51,fix_54,fix_55,fix_56,fix_58,fix_59,pido/
>
</MOVERS>
<APPLY_TO_POSE>
</APPLY_TO_POSE>
<PROTOCOLS>
    <Add mover_name=ala_pose/>
    <Add mover_name=ppk/>
    <Add mover_name=design/>
    <Add mover_name=dck/>
    <Add mover_name=design/>
    <Add mover_name=dck/>
    <Add mover_name=design/>
    <Add mover_name=dck/>
    <Add mover_name=design/>
    <Add filter_name=ddg_loose/>
    <Add filter_name=sasa/>
    <Add filter_name=unsat/>
</PROTOCOLS>
</dock_design>
```

The design run was launched ten times. The consensus sequence was chosen for experimental validation after minor manual modification (e.g. a less-represented amino acid amongst the set of ten designs may be substituted for the consensus residue based on user preference).

Computational methods: Seeded *ab initio* design of structural homologues (Fold From Loops)

Generate fragments that match the guiding scaffold's secondary structure
The amino acid sequence of the guiding scaffold (scaffold.fasta) was used to predict a secondary structure file in psipred_ss2 format (Jones, 1999). 3-mer and 9-mer fragments were then collected from the PDB to match the predicted secondary structure using the program NNMake, as described previously (Gront et al., 2011). Both psipred_ss2 and fragment files are generated with the command:

```
~directory_path/nnmake/make_fragments.pl –verbose scaffold.fasta
```

If the predicted secondary structure did not match the intended secondary structure, then the psipred_ss2 file was manually modified in a text editor to accurately reflect the known secondary structure of the guiding scaffold. Fragments were then generated with NNMake:

```
~directory_path/nnmake/make_fragments.pl -nosam -nojufo -noprof –verbose
scaffold.fasta
```

NNMake will search for a scaffold.psipred_ss2 file to match the scaffold.fasta file.

Loop file

The loop file specifies where in the guiding scaffold the motif will be positioned. For example, the contents of a loop file specifying placement of the Bim-BH3 motif between residues 48 and 61 is:

```
#LOOP start end cutpoint skip-rate extend
LOOP 48 61 0.0 X
```

Motif PDB file

A PDB file is required for the Bim-BH3 region that will act as the seed for folding. Backside residues that do not interact with BHRF1 were mutated to valine; these residues will be buried in the hydrophobic core of the designed protein and may be designed during protein assembly. For the design of BbpD04, nine side chains (Trp57, Ile58, Ala59, Leu62, Ile65, Gly66, Asp67, Phe69, and Asn70) of a fifteen-residue fragment (Bim a.a.56-70) were kept fixed, while remaining residues (Ile56, Gln60, Glu61, Arg63, Arg64, and Glu68) were mutated to valine and were available for design.

Fold From Loops (FFL) command line

Structural homologues of the guiding scaffold were assembled around the motif using the FFL application in the ROSETTA software suite (Correia et al., 2014):

```
/directory_path/fold_from_loops_devel.static.linuxiccrelease -database
/directory_path/minirosetta_database -s scaffold.pdb -loops::loop_file
loop_file_name -loops::frag_sizes 9 3 1 -in:file:frag9 9mers_fragment_file -
in:file:frag3 3mers_fragment_file -out::nstruct 5000 -out::file::silent
silent_file -fold_from_loops::swap_loops motif.pdb -
fold_from_loops::add_relax_cycles 2 -in::file::psipred_ss2
scaffold.psipred_ss2 -fold_from_loops::ca_rmsd_cutoff 5 -
out::file::silent_struct_type binary -fold_from_loops::native_ca_cst -
fold_from_loops::ca_csts_dev 3.0 -fold_from_loops::loop_mov_nterm 2 -
fold_from_loops::loop_mov_cterm 2 -abinitio::steal_3mers -
abinitio::steal_9mers -fold_from_loops::res_design_bs [list of residue #s in
the motif which can be designed; these will be on the backside of the motif
facing in to the core of the newly designed protein] -no_his_his_pairE
```

Interface Design

5,000-10,000 unique proteins were assembled using the FFL protocol. Interface design proceeded on only the lowest energy 1,000 structures. Each of the structures was superimposed to the Bim-BH3 peptide of crystal structure 2WH6 (Bim-BH3•BHRF1) via the incorporated Bim-BH3 motif, generating a docked configuration between the designed protein and BHRF1. A list was generated of the docked structure files. The surrounding interface outside the

incorporated Bim-BH3 motif was then designed using ROSETTA. Example command line and protocol are:

```
/directory_path/rosetta_scripts.static.linuxiccrelease -database
/directory_path/minirosetta_database/ -parser:protocol interface_design.xml -
l docked_poses.list -nstruct 1 -ntrials 5 -ignore_unrecognized_res -ex1 -ex2
-extrachi_cutoff 5 -hbond_fade 1.9 2.3 2.3 2.6 0.3 0.7 0.0 0.05 -
no_his_his_pairE

<dock_design>
<SCOREFXNS>
</SCOREFXNS>
<TASKOPERATIONS> These list the incorporated Bim-BH3 residues to remain fixed.
    <ProteinInterfaceDesign name=pido/>
    <PreventRepacking name=fix_W49 resnum=206/>
    <PreventRepacking name=fix_I50 resnum=207/>
    <PreventRepacking name=fix_A51 resnum=208/>
    <PreventRepacking name=fix_L54 resnum=211/>
    <PreventRepacking name=fix_I57 resnum=214/>
    <PreventRepacking name=fix_G58 resnum=215/>
    <PreventRepacking name=fix_D59 resnum=216/>
    <PreventRepacking name=fix_F61 resnum=218/>
    <PreventRepacking name=fix_N62 resnum=219/>
</TASKOPERATIONS>
<FILTERS>
    <Ddg name=ddg_loose scorefxn=score12 threshold=-2/>
    <Ddg name=ddg_strict scorefxn=score12 threshold=-15/>
    <Sasa name=sasa threshold=800/>
    <BuriedUnsatHbonds name=unsat cutoff=20/>
</FILTERS>
<MOVERS>
    <build_Ala_pose name=ala_pose partner1=0 partner2=1
task_operations=fix_W49,fix_I50,fix_A51,fix_L54,fix_I57,fix_G58,fix_D59,fix_F
61,fix_N62,pido/>
    <Prepack name=ppk scorefxn=score12 jump_number=0
task_operations=fix_W49,fix_I50,fix_A51,fix_L54,fix_I57,fix_G58,fix_D59,fix_F
61,fix_N62,pido/>
    <RepackMinimize name=design scorefxn_repack=score12
scorefxn_minimize=score12 repack_partner1=1 repack_partner2=1
design_partner1=0 design_partner2=1 interface_cutoff_distance=8.0
minimize_bb=1 minimize_rb=1 minimize_sc=1
task_operations=fix_W49,fix_I50,fix_A51,fix_L54,fix_I57,fix_G58,fix_D59,fix_F
61,fix_N62,pido/>
</MOVERS>
<APPLY_TO_POSE>
</APPLY_TO_POSE>
<PROTOCOLS>
    <Add mover_name=ala_pose/>
    <Add mover_name=ppk/>
    <Add filter_name=ddg_loose/>
    <Add mover_name=design/>
    <Add filter_name=ddg_strict/>
    <Add filter_name=sasa/>
    <Add filter_name=unsat/>
</PROTOCOLS>
</dock_design>
```

Filtering
Proteins that passed the interface design filters (buried SASA > 800 Å2, calculated ΔΔG < -15 REU, unsatisfied buried polar atoms < 20) were further filtered based on properties of the unbound designed protein. The lowest scoring 10-20 designs for monomer energy, unsatisfied buried polar atoms, and RosettaHoles score were selected for manual inspection. Designs were human modified to increase packing within the hydrophobic core and increase surface hydrophilicity, using the ROSETTA graphical user interface FoldIt (Cooper et al., 2010). Those designs considered most promising by the human eye were then selected for experimental validation.

For the 'direct-from-computer' designs tested in a high-throughput yeast display library (main Figure 1B), 5,000 structures were initially assembled using the FFL procedure. The lowest scoring 1,000 were designed at the interface, with 423 designs passing the minimum threshold for interface binding energy. From these 423, the 74 designs with the lowest number of buried unsatisfied hydrogen bonding atoms in the unbound monomer were chosen for experimental testing.

Other computational methods

Predicted binding probabilities for BbpD04 point mutants were calculated using the method of (Whitehead et al., 2012), with mutations ranked according to specificity improvements based on the electrostatics term in the score function. *Ab initio* structure prediction for forward folding of designed sequences is previously described (Rohl et al., 2004).

Plasmids, gene synthesis and mutagenesis

Genes encoding Bcl-2 proteins were synthesized (Genscript) and cloned with C-terminal avi-6his tags (GLNDIFEAQKIEWHEGSHHHHHH) into plasmid pET29b (NdeI-XhoI sites; Novagen): human Bcl-2 a.a. 1-207 (Accession No. NP_000624.2), Bcl-w a.a. 1-182 (AAB09055.1), Bfl-1 a.a. 1-153 (C4S mutation; NP_004040), Bcl-B a.a. 11-175 (NP_065129.1), Mcl-1 a.a. 172-327 (Q07820.3), Bcl-X_L a.a. 1-205 (CAA80661), and EBV BHRF1 a.a. 1-161 (YP_401646). For later BLI analysis, Bcl-B and Bfl-1 were genetically fused to the C-terminus of maltose-binding protein with an avi-6his tag for improved solution properties. Codon usage was optimized for *E. coli* expression. Human Bim-BH3 (a.a. 141-166, Accession No. O43521) was cloned into pETCON (NdeI-XhoI sites). The genes for individually-tested designed proteins were assembled from oligos (Hoover and Lubkowski, 2002) and cloned into pET29b (NdeI-XhoI sites) with C-terminal 6his tags for purification from *E. coli*, or cloned into pETCON (NdeI-XhoI sites) for yeast surface expression. Alternative tags were added using PCR methods. Point mutations were made by overlapping PCR (Procko et al., 2013). Error-prone PCR with an average error rate of 1.3 amino acid substitutions per clone used GeneMorph II Random Mutagenesis (Agilent Technologies).

Protein purification

E. coli BL21* (DE3) (Invitrogen) transformed with the relevant plasmid were grown at 37 ºC in terrific broth with 50 µg/ml kanamycin to OD_{600} 0.5-0.8, transferred to 21 ºC and expression induced overnight with 0.1 mM IPTG. Centrifuged cells were resuspended in lysis buffer (20 mM Tris-Cl pH 8.0, 20 mM imidazole, 300 mM NaCl, 0.5 mM PMSF) supplemented with 0.2 mg/ml lysozyme and 0.06 mg/ml DNase I, and sonicated. Cleared lysate was incubated with NiNTA-agarose at 4 ºC for 1 h and collected in a chromatography column. The resin was washed with 100 column volumes (CV) lysis buffer and protein was eluted with 6 CV elution buffer (20 mM Tris-Cl pH 8.0, 250 mM imidazole, 300 mM NaCl, 0.5 mM PMSF, 0.05% β-mercaptoethanol). Proteins were concentrated using a centrifugal ultrafiltration device (Sartorius) and separated from remaining contaminants by SEC using a Sephacryl-100 16/600 column (GE Healthcare) with running buffer (20 mM Tris-Cl pH 7.5, 150 mM NaCl, 1 mM DTT). Fractions containing pure protein were pooled, concentrated to 5-20 mg/ml based on calculated extinction coefficients for absorbance at 280 nm, and aliquots snap frozen in liquid N_2 for storage at -80 ºC. For animal studies, endotoxin was removed with a high-capacity endotoxin removal spin column (Pierce) and reducing agent was removed with a PD-10 desalting column (GE Healthcare).

Enzymatic ligand biotinylation

Purified avi-6his-tagged ligands (20 µM) in reaction buffer (250 mM potassium glutamate, 20 mM Tris-Cl [pH 7.5], 50 mM bicine [pH 8.3], 10 mM ATP, 10 mM MgOAc, 100 µM d-biotin) were enzymatically biotinylated with 150 U/µl BirA (Avidity) at room temperature overnight, followed by purification with NiNTA-agarose and SEC. Biotinylated ligands were stored at 4 ºC in 150 mM NaCl, 20 mM Tris-Cl (pH 7.5), 1 mM DTT, 0.02% sodium azide.

Yeast surface display

Transformed EBY100 yeast were cultured, induced and binding of surface displayed protein to biotinylated ligands was assessed by flow cytometry as reported (Chao et al., 2006; Procko et al., 2013). All yeast displayed proteins had C-terminal *myc* epitope tags for detection with FITC-conjugated anti-myc (Immunology Consultants Laboratory). Binding of biotinylated protein to the yeast surface is detected with phycoerythrin-conjugated streptavidin (Invitrogen).

Deep sequencing analysis

Yeast cells were sorted on a BD Influx cytometer operated by Spigot (BD Biosciences) and recovered in SDCAA media at 30 ºC overnight. Yeast were lysed with 125 U/ml Zymolase at 37 ºC for 5 h, and DNA was harvested (Zymoprep kit from Zymo Research). Genomic DNA was digested with 2 U/µl Exonuclease I and 0.25 U/µl Lambda exonuclease (New England Biolabs) for 90 min at 30 ºC, and plasmid DNA purified with a QIAquick kit (Qiagen). DNA was deep sequenced with a MiSeq sequencer (Illumina) and sequences were analyzed with adapted scripts from Enrich (Fowler et al., 2011).

For the library of designs in main Figure 1B, genes were synthesized (Gen9) with barcodes downstream of the stop codon for easy identification during deep sequencing (Table S3). After yeast cell transformation (6×10^5 transformants), expression, sorting and plasmid DNA purification, the genes were PCR amplified using primers that annealed to external regions

within the plasmid (primer sequences available upon request), followed by a second round of PCR to add flanking sequences for annealing to the Illumina flow cell oligonucleotides and a 6-bp sample identification sequence. PCR rounds were 12 cycles each with high-fidelity Phusion polymerase (New England Biolabs). Barcodes were read on a MiSeq sequencer using a 50-cycle reagent kit (Illumina). 257,812 sequences passing the chastity filter were read in the naive population (ranging from 260 to 17,192 reads per gene, with a median of 2,492). The sorted populations had 117,720 to 232,195 reads.

For the single-site saturation mutagenesis library (main Figure 2; library contained 2.5×10^6 transformants), plasmid DNA was purified from the pre- and post-sorted populations, and the BbpD04.3 gene was amplified as two overlapping fragments to provide complete sequencing coverage. Additional flanking DNA for annealing to the Illumina flow cell was added by PCR as described above. Gel-purified DNA was sequenced on a MiSeq sequencer using a 300-cycle paired-end reads reagent kit (Illumina). 3,058,244 sequences passing the chastity filter were read for the naive population. Each single amino acid substitution had 10 to 10,856 reads, with a median of 451 reads per mutant, and only mutation E109F was not represented. Parental protein sequences accounted for ~25% of reads. 2,930,499 and 2,548,997 sequences passing the chastity filter were read for the affinity and affinity-specificity sorted populations, respectively.

Analytical size exclusion chromatography

Proteins (20 nmol each) were injected in a 200 µl loop in line with a Superdex-75 10/300 column (GE Healthcare) and separated with running buffer (20 mM Tris-Cl pH 7.5, 150 mM NaCl, 1 mM DTT) at room temperature.

Crystallography

A complex of untagged BINDI and C-terminal 6his-BHRF1 was co-purified from *E. coli* lysate via Ni-NTA metal affinity chromatography. The protein was further purified by SEC (running buffer: 20 mM Tris-Cl pH 7.5, 150 mM NaCl, 1 mM DTT) and concentrated to 22 mg/ml. Crystal clusters were grown by vapor diffusion after mixing 1:1 drops of protein with reservoir (8-12% PEG8000, 100 mM Tris-Cl pH 8.5, 200 mM $MgCl_2$). Clusters were broken into fragments that were cryopreserved with 18-20 % glycerol in mother liquid prior to flash freezing. Two datasets were collected; one using a Rigaku MicroMax-007HF rotating anode generator equipped with a Saturn CCD detector, the second from beam line BL 5.0.2 at the Advanced Light Source at Lawrence Berkeley National Laboratory. Datasets were integrated and scaled using HKL2000 (Otwinowski and Minor, 1997). Molecular replacement used PHASER (McCoy et al., 2007) with chain A of PDB 2WH6 and a computational model of BINDI. Model building was with COOT (Emsley and Cowtan, 2004) and refinement used Refmac5 (Skubak et al., 2004).

Proteolysis susceptibility assay

Substrates (0.5 mg/ml) were incubated at 37°C with protease (0.01 mg/ml) in 50 mM Tris-HCl (pH 8.0), 10 mM $CaCl_2$. Reactions were terminated with benzamidine (12.5 mM final), PMSF

(1.25 mM final) and 4× load dye. Samples were run on 18% SDS-polyacrylamide gels, and stained with Coomassie dye.

Circular dichroism

CD spectra were recorded with a Model 420 spectrometer (AVIV Biomedical). Unless stated otherwise, proteins were at 10 μM in PBS and data were collected at 25°C.

Bio-layer interferometry

Data were collected on an Octet RED96 (Forte Bio) and processed using the instrument's integrated software. Enzymatically-biotinylated Bcl-2 proteins (25 nM) in binding buffer (10 mM HEPES [pH 7.4], 150 mM NaCl, 3 mM EDTA, 0.05% surfactant P20, 0.5% non-fat dry milk) were immobilized for 360 s at 30 ºC to streptavidin biosensors. Biosensors were dipped in solutions containing the analyte of interest to measure association, and transferred back to empty binding buffer for monitoring dissociation. Kinetic constants were determined from the mathematical fit of a 1:1 binding model.

Peptide synthesis

Bim-BH3 peptide (sequence Ac-CMRPEIWIAQELRRIGDEFNAYYARR-ON) was synthesized by Fmoc solid phase synthesis on a PS3 (Protein Technologies) using Rink Amide-MBHA resin (EMD Millipore). Peptide was purified by RP-HPLC on a Jupiter 5 μm C18 300Å column (Phenomenex) with an Agilent 1260 HPLC and confirmed by ion trap mass spectrometry with electrospray.

Cytochrome c release

Cells (~10^9) were equilibrated in 5 ml of homogenization buffer (0.25 M sucrose, 1 mM EGTA, 10 mM HEPES/NaOH, 0.5% BSA, pH 7.4, Roche Complete protease inhibitors) for 5 min. Samples were kept on ice or at 4 ºC until assayed. Cells were homogenized under N_2 pressure (400 psi) in a steel disruption vessel (Parr Instrument Company) for 10 min, then centrifuged (750 g) for 10 min to remove intact cells. Supernatant was centrifuged again (12,000 g) for 12 min to collect mitochondria. The pellet was resuspended in 300 μl wash buffer (0.25 M sucrose, 1 mM EDTA, 10 mM Tris/HCl pH 7.4). Proteins at the indicated concentrations were incubated with mitochondria (25 μg mitochondrial protein based on BCA assay, Sigma) in 50 μl final volume of experimental buffer (125 mM KCl, 10 mM Tris-MOPS pH 7.4, 5 mM glutamate, 2.5 mM malate, 1 mM K-PO_4, 10 μM EGTA-Tris pH 7.4) for 30 min at room temperature. Reaction solutions were centrifuged (18,000 g) for 10 min at 4 ºC and cytochrome c release was quantified using a Cytochrome c ELISA kit (Life Technologies). Complete cytochrome c release was quantified by treatment with 0.5% Triton-X100.

Cell viability assay

A 25,000 Da diblock copolymer (Pol300) composed of 95% polyethylene glycol methacrylate (300 Da) for stability and 5% pyridyl disulfide methacryate for conjugation in the first block, and

60% diethylaminoethyl methacrylate and 40% butyl methacrylate in the second block, was synthesized by reversible addition-fragmentation chain transfer. Development and characterization of the Pol300 diblock copolymer will be published in a separate article. After purification, Pol300 was dissolved in ethanol at 100 mg/ml then diluted into PBS at 10 mg/ml and spin filtered to remove ethanol. Proteins with exposed terminal cysteines were incubated with Pol300 at a molar ratio of 2:1 (protein:polymer) overnight. Protein-copolymer conjugation was quantified by measuring pyridyl disulfide release and the absorbance of 2-mercaptopyridine at 343 nm with 8,080 $M^{-1}cm^{-1}$ as the extinction coefficient. For cell viability studies, protein and protein-polymer conjugates were incubated with Ramos or Ramos-AW cells in a 96 well round bottom plate with 50,000 cells per well in 100 µl media. After 24 h, cell viability was measured using a CellTiter 96 Aqueous One Solution Cell Proliferation Assay, MTS (Promega).

Reverse transcription-PCR

RNA was extracted from cells using the Qiagen Qiashredder and Qiagen RNeasy Mini Kits, as per manufacturer's directions. First-strand cDNA was synthesized with Superscript III RT (Life Technologies) using 2 µg total RNA in a 20 µl reaction volume. The product was diluted 1:10, and 1 µl used as the template (25 µl total reaction volume) for PCR amplification using GoTaq Green Master Mix (Promega). Primer sequences for amplifying fragments of BHRF1 and GAPDH are available upon request.

Tissue culture

Ramos, Ramos-AW, Daudi, Raji, DOHH2, JVM-2, and JVM-13 were grown in RPMI 1640 containing L-glutamine and 25 mM HEPES supplemented with 1% penicillin-streptomycin (GIBCO) and 10% fetal bovine serum (FBS, Invitrogen). Jeko-1 were grown in similar RPMI 1640 media supplemented with 20% FBS. Granta-519 and K562 were grown in Iscove's DMEM supplemented with 10% FBS. All cell lines were maintained in log growth phase at 37 °C and 5% CO_2.

Xenograft mouse model

To prepare mAb-copolymer-protein conjugates, a 44,000 Da diblock copolymer (Pol950) composed of 80% polyethylene glycol methacrylate (950 Da), 10% pyridyl disulfide methacrylate, and 10 % biotin-hydroxyethyl methacrylate for mAb-streptavidin conjugation in the first block, and 60% diethylaminoethyl methacrylate and 40% butyl methacrylate in the second block, was synthesized by reversible addition-fragmentation chain transfer. The full synthesis, development and pharmaceutical properties of the Pol950 diblock copolymer will be published in a separate article. Pol950 was dissolved in ethanol at 100 mg/mL, then diluted in PBS at 10 mg/ml and spin filtered to remove ethanol. Proteins were incubated with Pol950 at an equimolar ratio overnight and conjugation was quantified by A_{343} absorbance. αCD19 (human monoclonal CAT-13.1E10-SA) was conjugated to protein-poylmer through the streptavidin linkage at a molar ratio of 90:1 (polymer:mAb).

BALB/c nu/nu mice (6 to 8 weeks old) were used from Harian Sprague-Dawley and housed under protocols approved by the FHCRC Institutional Animal Care and Use Committee. Mice

were placed on biotin-free diet (Purina Feed) for the duration of study. To form tumor-xenografts, Ramos-AW cells were resuspended in PBS (5×10^7 cells/mL) and injected in the right flank with 10^7 cells/mouse. Tumors were allowed to grow for 6 days to a volume of 50 mm^3. Mice with similar sized tumors were sorted randomly into treatment groups (n = 8 to 10). On days 6, 9, and 12, mice were injected intraperitoneally with cyclophosphamide (35 mg/kg) and bortezomib (0.5 mg/kg). After 30 min, mice were injected via tail vein with conjugates at a dose of 15 mg/kg (αCD19), 300 mg/kg (Pol950) and 105 mg/kg (BINDI or 3LHP). Body weight was monitored for toxicity and tumor sizes were measured while blinded to treatment groups. Measurements were performed in the x, y, and z plane using calipers three times a week. Mice were euthanized when tumors reached a volume of 1250 mm^3. Tumor volumes and deaths were recorded into Prism (GraphPad Software, Inc.) for statistical analysis and a log-rank (Mantel-Cox) test was performed to determine if survival curves and trends were statistically different ($P < 0.0001$). Significance in tumor volumes was verified by an unpaired t test with Welch's correction.

SUPPLEMENTAL REFERENCES

Chao, G., Lau, W. L., Hackel, B. J., Sazinsky, S. L., Lippow, S. M., and Wittrup, K. D. (2006). Isolating and engineering human antibodies using yeast surface display. Nat Protoc *1*, 755-768.

Cooper, S., Khatib, F., Treuille, A., Barbero, J., Lee, J., Beenen, M., Leaver-Fay, A., Baker, D., Popovic, Z., and Players, F. (2010). Predicting protein structures with a multiplayer online game. Nature *466*, 756-760.

Emsley, P., and Cowtan, K. (2004). Coot: model-building tools for molecular graphics. Acta Crystallogr D Biol Crystallogr *60*, 2126-2132.

Fleishman, S. J., Leaver-Fay, A., Corn, J. E., Strauch, E. M., Khare, S. D., Koga, N., Ashworth, J., Murphy, P., Richter, F., Lemmon, G., *et al.* (2011b). RosettaScripts: a scripting language interface to the Rosetta macromolecular modeling suite. PLoS One *6*, e20161.

Fowler, D. M., Araya, C. L., Gerard, W., and Fields, S. (2011). Enrich: software for analysis of protein function by enrichment and depletion of variants. Bioinformatics *27*, 3430-3431.

Gront, D., Kulp, D. W., Vernon, R. M., Strauss, C. E., and Baker, D. (2011). Generalized fragment picking in Rosetta: design, protocols and applications. PLoS One *6*, e23294.

Hoover, D. M., and Lubkowski, J. (2002). DNAWorks: an automated method for designing oligonucleotides for PCR-based gene synthesis. Nucleic Acids Res *30*, e43.

Jones, D. T. (1999). Protein secondary structure prediction based on position-specific scoring matrices. J Mol Biol *292*, 195-202.

McCoy, A. J., Grosse-Kunstleve, R. W., Adams, P. D., Winn, M. D., Storoni, L. C., and Read, R. J. (2007). Phaser crystallographic software. J Appl Crystallogr *40*, 658-674.

Otwinowski, Z., and Minor, M. (1997). Processing of X-ray Diffraction Data Collected in Oscillation Mode. In Macromolecular Crystallography, part A, C. W. Carter Jr, and R. M. Sweet, eds. (Academic Press), pp. 307-326.

Rohl, C. A., Strauss, C. E., Misura, K. M., and Baker, D. (2004). Protein structure prediction using Rosetta. Methods Enzymol *383*, 66-93.

Skubak, P., Murshudov, G. N., and Pannu, N. S. (2004). Direct incorporation of experimental phase information in model refinement. Acta Crystallogr D Biol Crystallogr *60*, 2196-2201.

Whitehead, T. A., Chevalier, A., Song, Y., Dreyfus, C., Fleishman, S. J., De Mattos, C., Myers, C. A., Kamisetty, H., Blair, P., Wilson, I. A., and Baker, D. (2012). Optimization of affinity, specificity and function of designed influenza inhibitors using deep sequencing. Nat Biotechnol *30*, 543-548.

Supplemental Figure S1

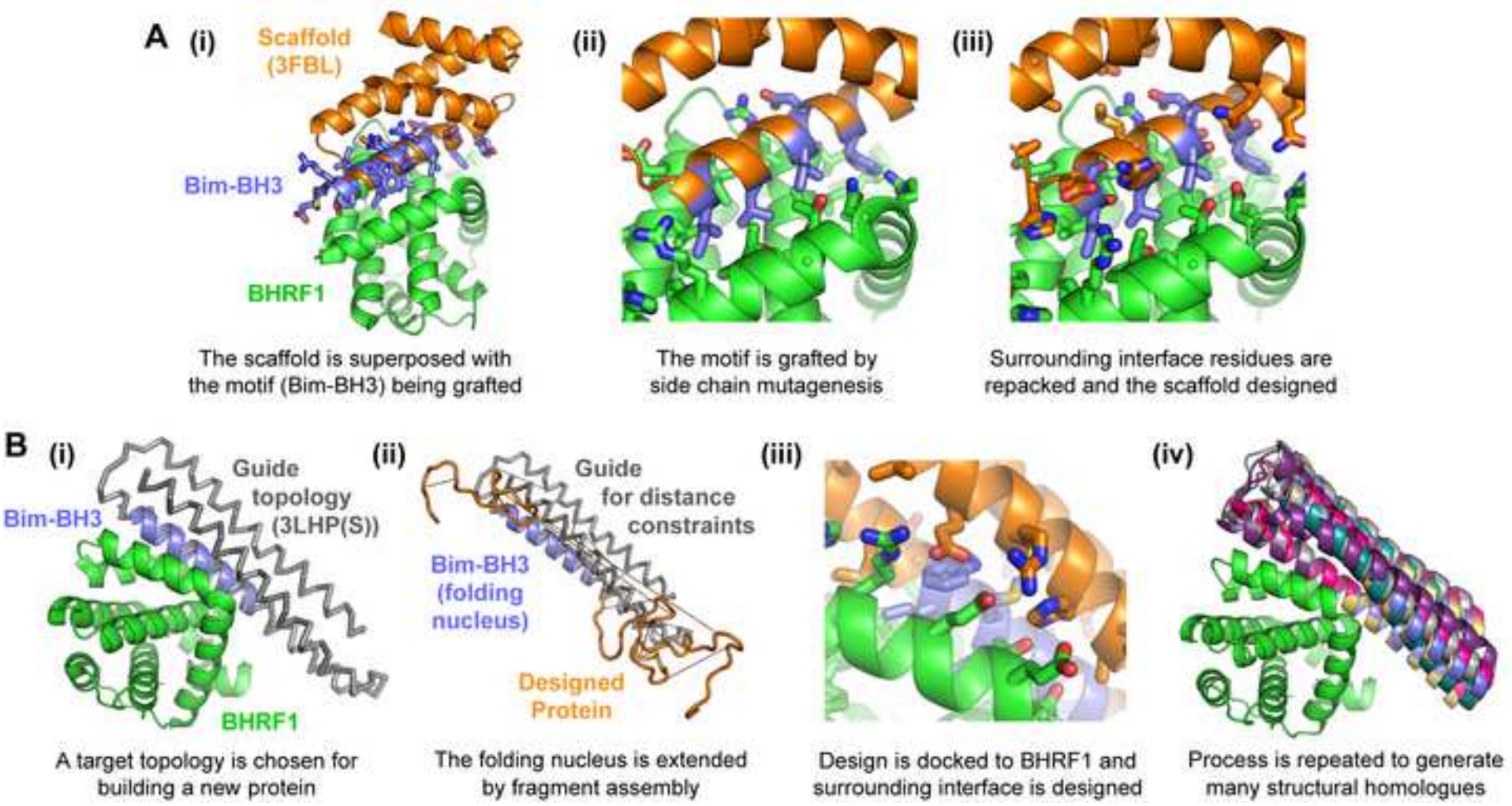

Supplemental Figure S2

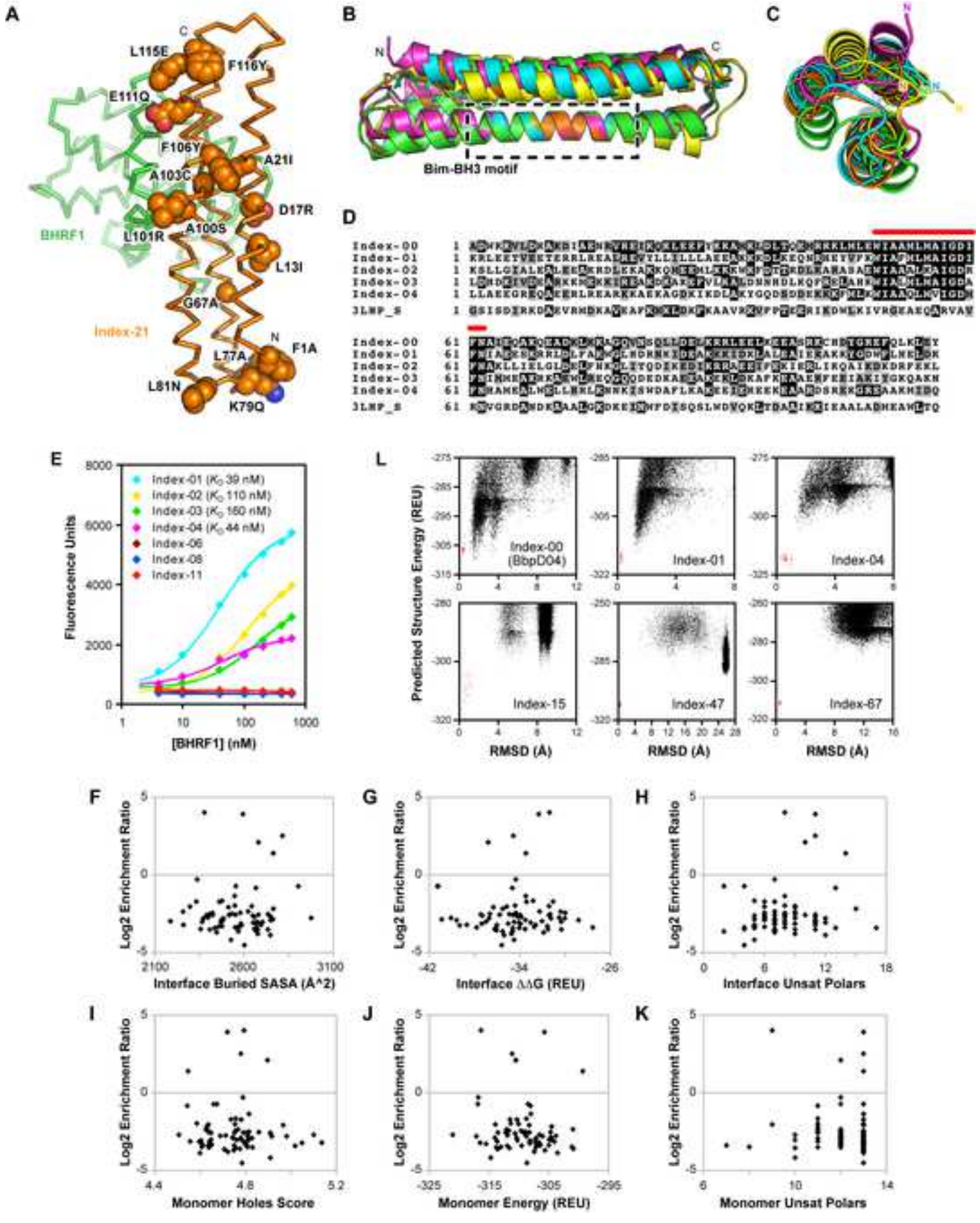

Supplemental Figure S3

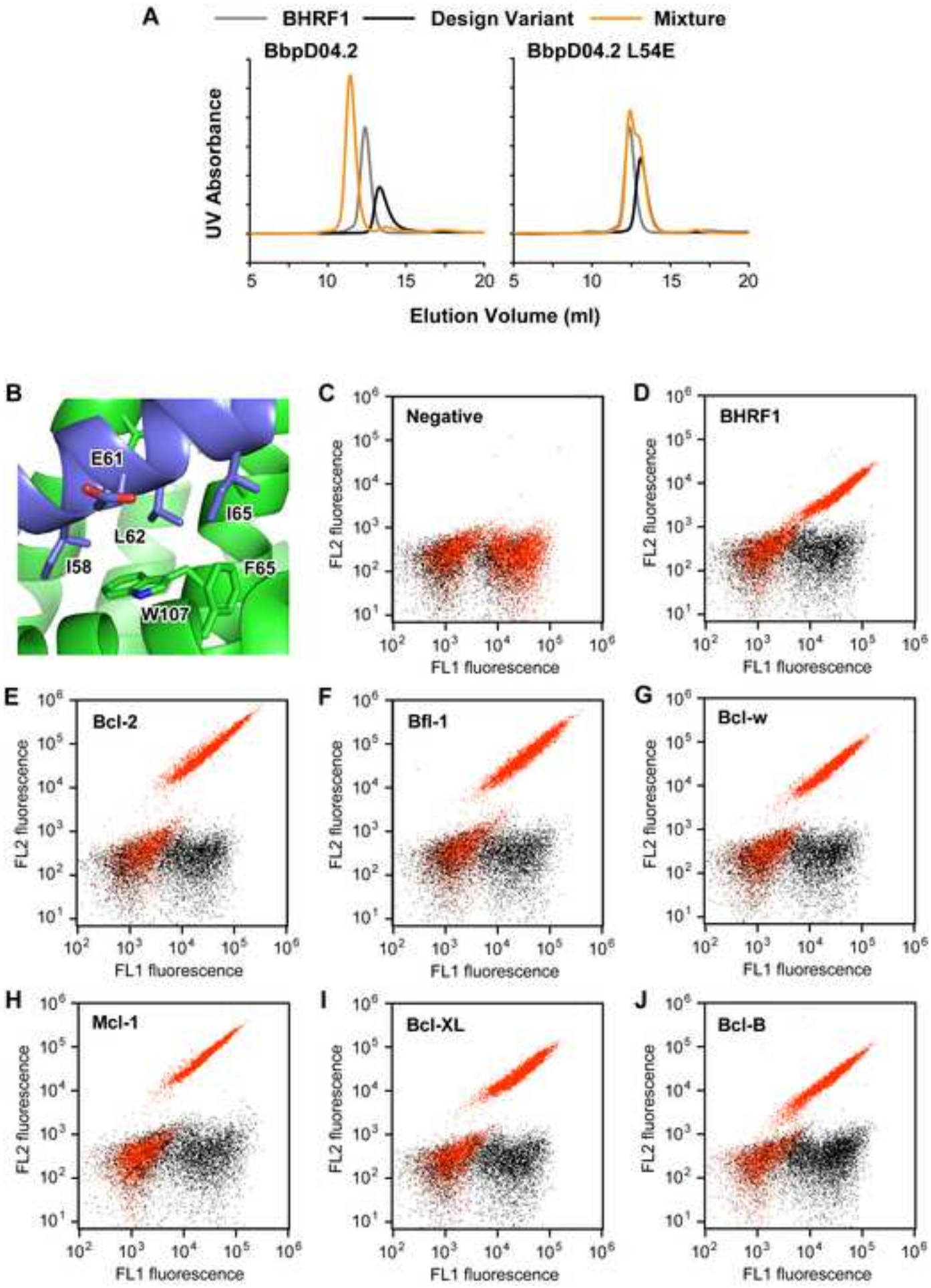

Supplemental Figure S4

A

	N-terminus	C-terminus
Linker -0	M	LEHHHHHH
Linker -1	MGSCA	LEHHHHHH
Linker -2	MSGHHHHHHGS	SGCAE
Linker -3	MSGHHHHHHGS	SSGDSGCAE
Linker -4	M	SEHHHHHHGSCE

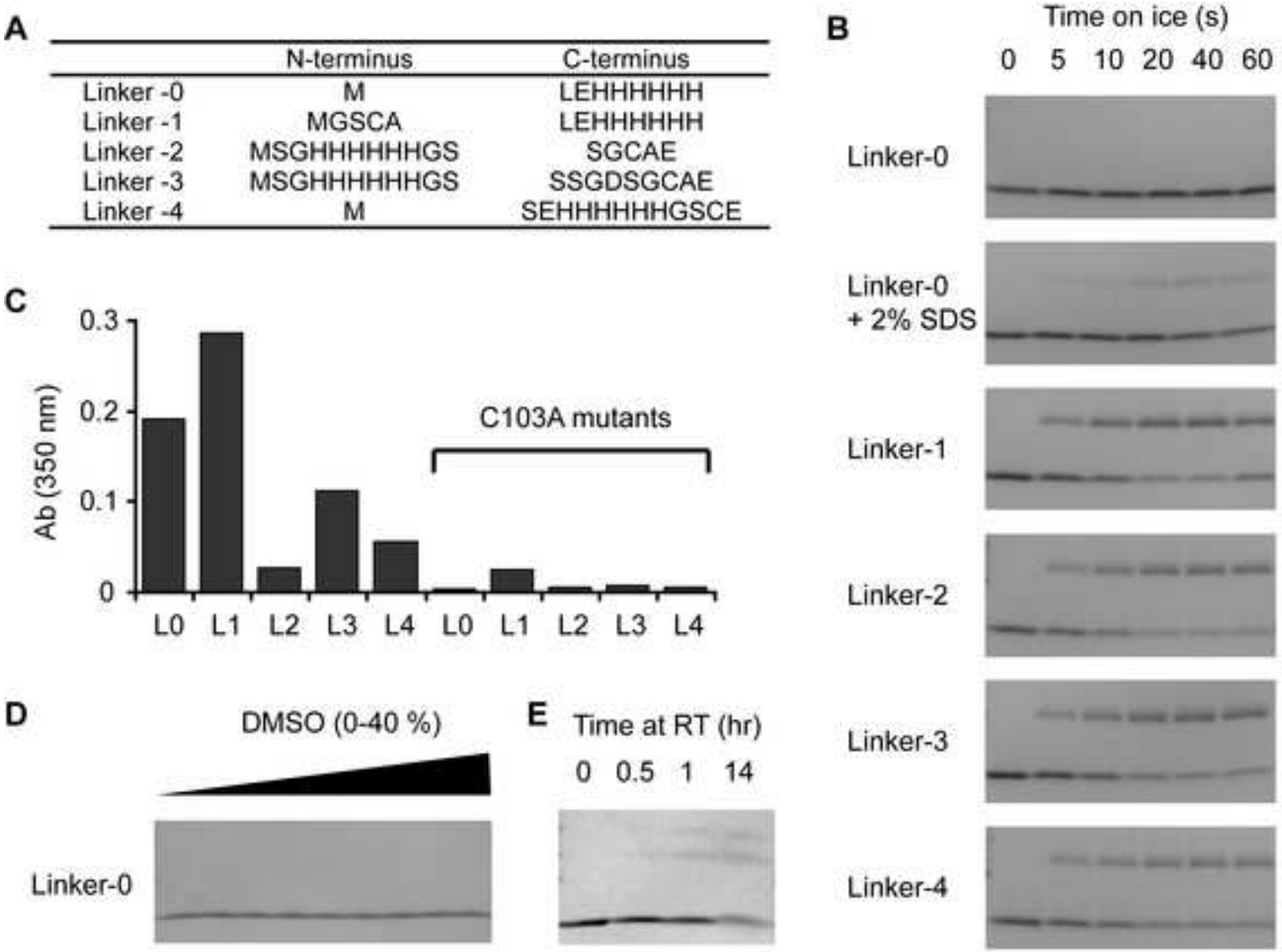

F

Protein	Apparent binding constants for prosurvival Bcl-2 family members (nM; mean ± SE, n = 3-6)						
	BHRF1	Bcl-2	Bcl-W	Mcl-1	Bfl-1	Bcl-XL	Bcl-B
BbpD04.2	0.6 ± 0.2	33 ± 4	40 ± 10	26 ± 4	70 ± 20	31 ± 2	–
BbpD04.2 C103A (BbpD04.3)	0.54 ± 0.01	20 ± 2	34 ± 3	19 ± 1	32 ± 6	34 ± 7	–
BbpD04.2 C103V	0.62 ± 0.08	12.6 ± 0.9	9.6 ± 0.7	2.3 ± 0.1	19 ± 2	20 ± 3	–

Supplemental Figure S5

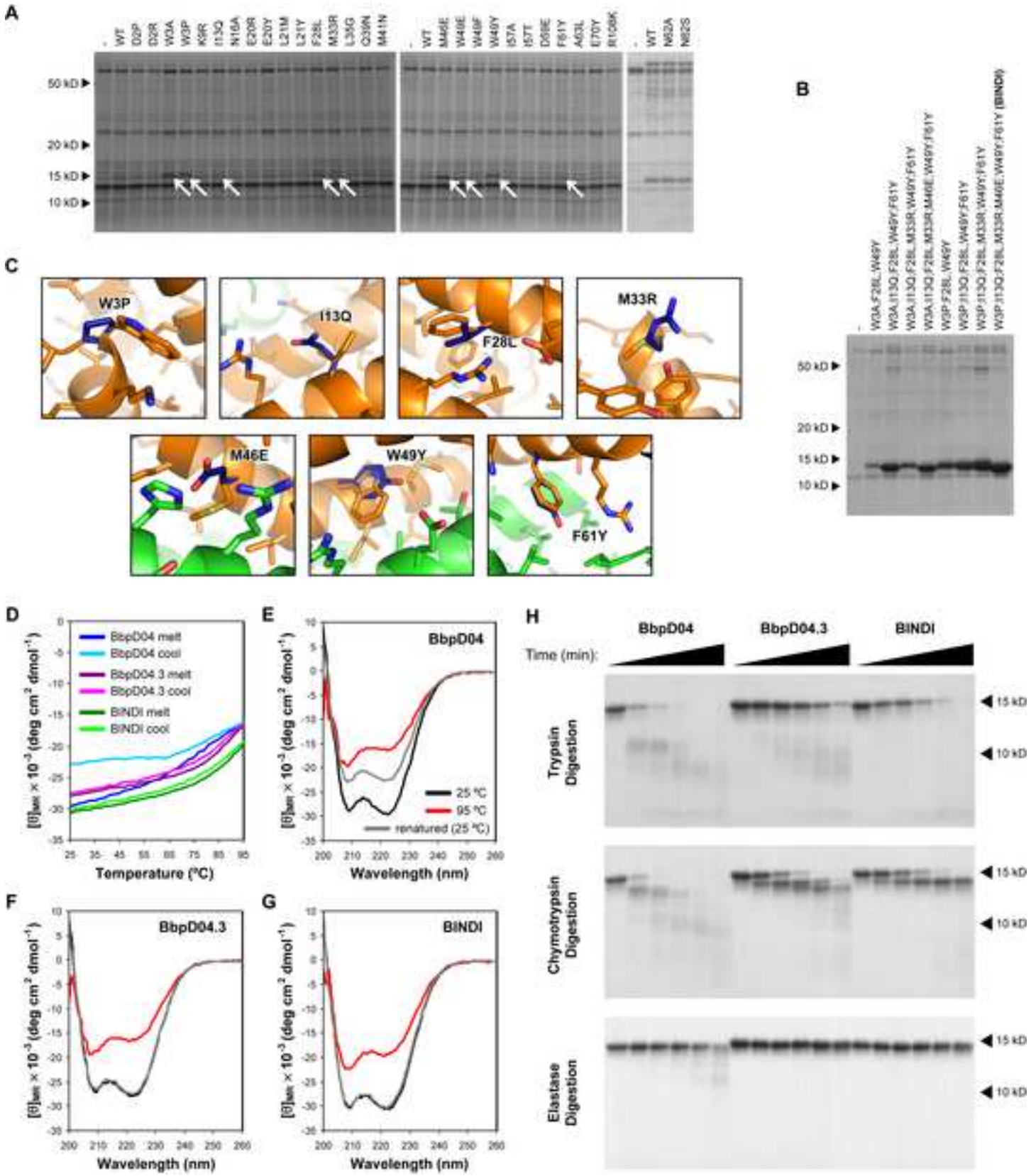

Supplemental Figure S6

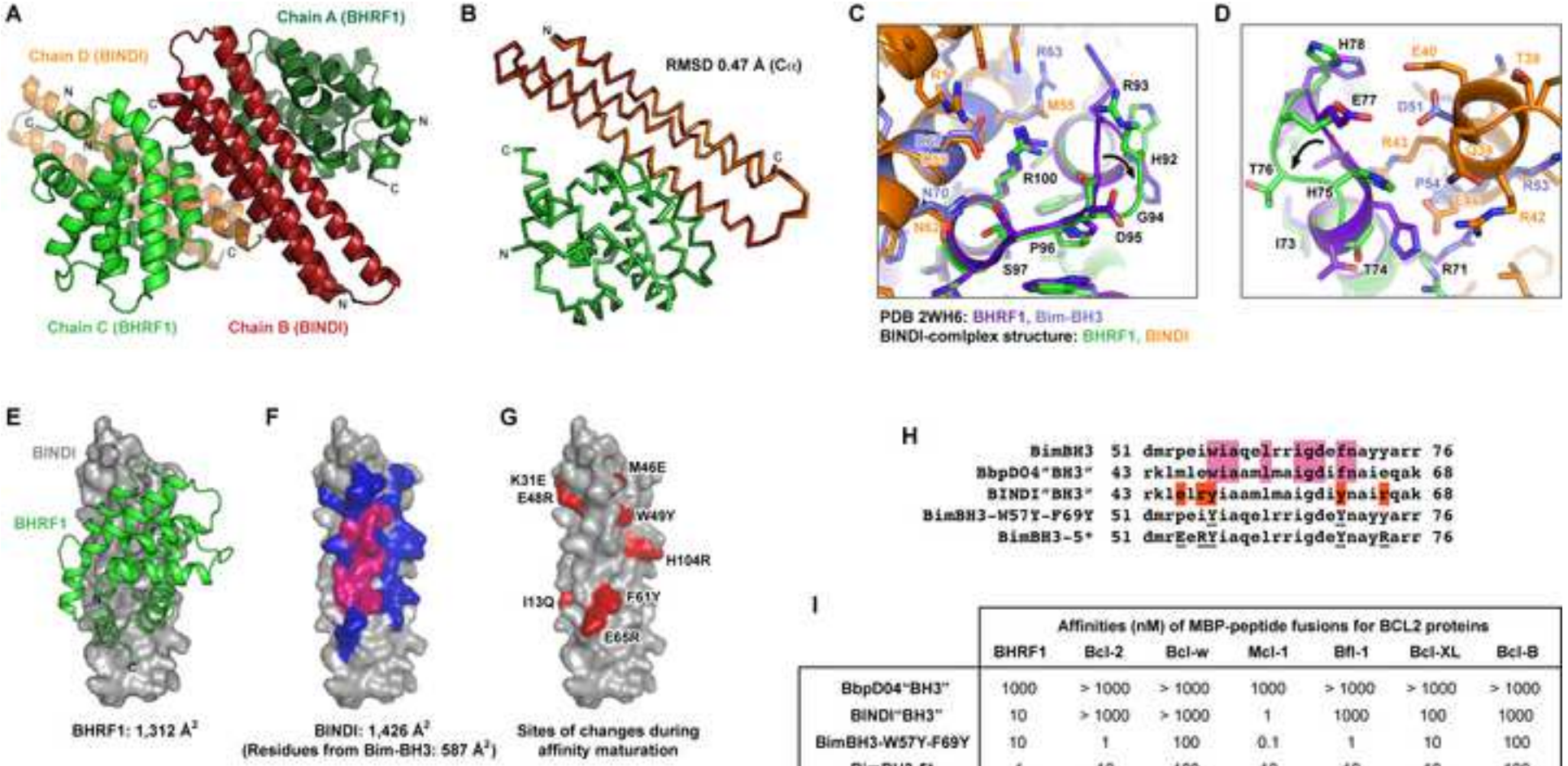

H

```
BimBH3          51 dmrpeiwiaqelrrigdefnayyarr 76
BbpD04"BH3"     43 rklmlewiaamlmaigdifnaieqak 68
BINDI"BH3"      43 rklelryiaamlmaigdiynairqak 68
BimBH3-W57Y-F69Y 51 dmrpeiYiaqelrrigdeYnayyarr 76
BimBH3-5*       51 dmrEeRYiaqelrrigdeYnayRarr 76
```

I

	Affinities (nM) of MBP-peptide fusions for BCL2 proteins						
	BHRF1	Bcl-2	Bcl-w	Mcl-1	Bfl-1	Bcl-XL	Bcl-B
BbpD04"BH3"	1000	> 1000	> 1000	1000	> 1000	> 1000	> 1000
BINDI"BH3"	10	> 1000	> 1000	1	1000	100	1000
BimBH3-W57Y-F69Y	10	1	100	0.1	1	10	100
BimBH3-5*	1	10	100	10	10	10	100

Supplemental Figure S7